Received: 24 May 2024 | Revised: 18 July 2024 | Accepted: 14 August 2024

DOI: 10.1002/mrm.30281

RESEARCH ARTICLE

Magnetic Resonance in Medicine

T1 and T2 measurements across multiple 0.55T MRI systems using open-source vendor-neutral sequences

Kathryn E. Keenan[1] | **Bilal Tasdelen**[2] | **Ahsan Javed**[3] | **Rajiv Ramasawmy**[3] | **Rudy Rizzo**[4] | **Michele N. Martin**[1] | **Karl F. Stupic**[1] | **Nicole Seiberlich**[4] | **Adrienne E. Campbell-Washburn**[3] | **Krishna S. Nayak**[2]

[1]National Institute of Standards and Technology, Boulder, Colorado, USA

[2]Ming Hsieh Department of Electrical and Computer Engineering, University of Southern California, Los Angeles, California, USA

[3]Cardiovascular Branch, Division of Intramural Research, National Heart, Lung, Blood Institute, National Institutes of Health, Bethesda, Maryland, USA

[4]Department of Radiology, University of Michigan, Ann Arbor, Michigan, USA

Correspondence
Kathryn E. Keenan, National Institute of Standards and Technology, Boulder, CO, USA.
Email: kathryn.keenan@nist.gov

Funding information
National Science Foundation, Grant/Award Number: 1828736; National Institutes of Health, Intramural Research Program, National Heart Lung and Blood Institute, Grant/Award Number: Z01-HL006257

Abstract

Purpose: To compare T1 and T2 measurements across commercial and prototype 0.55T MRI systems in both phantom and healthy participants using the same vendor-neutral pulse sequences, reconstruction, and analysis methods.

Methods: Standard spin echo measurements and abbreviated protocol measurements of T1, B1, and T2 were made on two prototype 0.55 T systems and two commercial 0.55T systems using an ISMRM/NIST system phantom. Additionally, five healthy participants were imaged at each system using the abbreviated protocol for T1, B1, and T2 measurement. The phantom measurements were compared to NMR-based reference measurements to determine accuracy, and both phantom and in vivo measurements were compared to assess reproducibility and differences between the prototype and commercial systems.

Results: Vendor-neutral sequences were implemented across all four systems, and the code for pulse sequences and reconstruction is freely available. For participants, there was no difference in the mean T1 and T2 relaxation times between the prototype and commercial systems. In the phantom, there were no significant differences between the prototype and commercial systems for T1 and T2 measurements using the abbreviated protocol.

Conclusion: Quantitative T1 and T2 measurements at 0.55T in phantom and healthy participants are not statistically different across the prototype and commercial systems.

KEYWORDS

0.55T, multi-site repeatability, T1, T2

1 | INTRODUCTION

T1 and T2 relaxation times are representative of physical processes. Given that, if the same measurement is made across multiple systems at the same field strength, the measured values should be the same. However, quantitative values vary with measurement method and

the experimental acquisitions, reconstructions, and signal modelling must be matched to result in the same measured values. Moreover, these measurements are hardware-dependent, and MRI hardware typically goes through prototype and upgrade cycles as technology advances. As a result, multi-system studies may need to incorporate different hardware and software platforms, even when the systems are from the same manufacturer.

Here, we are specifically investigating measurements across contemporary 0.55T MRI systems, in light of the recent commercialization. It is valuable to characterize these new systems across multiple sites, and to compare with predecessor prototype systems that were "ramped down" from 1.5 to 0.55T, for which much of the preliminary quantitative data has been reported.[1,2] The prototype 0.55T systems have higher-performance gradients, different numbers and layouts of RF coils, and a different bore geometry compared to the commercial 0.55T design. In theory, measurements of quantitative NMR parameters including T1 and T2 relaxation times made on the prototype 0.55T systems should be the same as measurements from the commercial 0.55T systems; however, differences between the design and capabilities of these two systems may lead to variations in measurement values.

Two studies of T1 measurement using closely matched systems (same or similar hardware, software, and pulse sequences) demonstrated high repeatability across the systems.[3,4] To achieve these, it was necessary to compare and harmonize pulse sequence code line-by-line across these systems. Other studies using unmatched sequences have been performed to compare relaxometry measurements across systems and sites, and the results are varied.[5–8] For T1 measurement, the largest differences are typically observed between systems from different vendors, rather than across systems of the same vendor. This has been shown in both phantom[9,10] and in vivo studies.[9,11] The other factors in multi-site T1 measurement differences are the specific sequence implementation[5–7] and software version.[5] Additionally, T1 measurement differences are observed following hardware and software upgrades.[8] T2 measurement is arguably more challenging since it is biased by B1+ and B0 inaccuracies that cannot be easily corrected.[12–14] A survey of myocardial T2 relaxation times reported in healthy adults found the reported values were dependent on vendor and pulse sequence.[15]

To use T1 and T2 measurements clinically as a diagnostic tool, it is necessary to replicate measurements across systems. Tools have been developed to enable the same experiment across systems and for the implementation of the same post-processing pipelines. Karakuzu et al. used RTHawk and qMRLab to develop a vendor-neutral pulse sequence and analysis workflow.[16] The vendor-neutral workflow significantly reduced inter-vendor T1 measurement differences in phantoms and in vivo. An international T1 mapping challenge demonstrated that open and harmonized acquisition and reconstruction is essential to obtain reproducible quantitative results, even more so when multi-site studies of the same or similar subjects are considered.[9] One tool for this purpose is Pulseq (https://pulseq.github.io/), an open-source vendor-agnostic pulse sequence programming environment, which can be used to develop and execute MRI pulse sequences across different vendor systems and platforms. Pulseq was used to implement the same acquisitions across different systems, including different platforms.[17–20]

In this study, we use Pulseq to implement the same pulse sequences for T1 and T2 measurements across commercial and prototype 0.55T MRI systems. We compare the measurements using both the ISMRM/NIST system phantom and healthy participants.

2 | METHODS

Measurements were made on two prototype 0.55T systems and two commercial 0.55T systems. On each system, prior to the study timeframe, protocols were validated using an ISMRM/NIST system phantom (CaliberMRI, Boulder, CO, USA); this system qualification data are not reported. Following this validation step, healthy participants were imaged, and phantom measurements were completed on each system. The goal was to complete all measurements (phantom and participants) within a 2-wk study time frame. The phantom measurements were compared to NMR-based reference measurements to determine accuracy, and both phantom and in vivo measurements were compared to assess reproducibility and differences between the prototype and commercial systems.

2.1 | Phantom measurements

A single ISMRM/NIST system phantom was shipped between the four different systems. The ISMRM/NIST system phantom includes $NiCl_2$ and $MnCl_2$ concentration arrays each containing 14 vials with a range of T1/T2 relaxation time combinations. The temperature of the phantom before and after imaging along with the ambient room temperature was measured using a thermometer provided with the phantom.

On the prototype systems, the system phantom measurements were acquired using a 12-element head and neck coil. On the commercial 0.55T systems, the head coil has a smaller diameter, and instead the system phantom was placed on the spine coil, and then the large flexible

TABLE 1 Pulse sequence details.

	Abbreviated			Standard spin echo		NMR-reference	
Parameter	**T1-mapping**	**B1-mapping**	**T2-mapping**	**T1-mapping**	**T2-mapping**	**T1-NMR**	**T2-NMR**
Sequence	3D VFA-GRE	3D AFI-GRE	MCSE	IRSE	SESE	Inversion Recovery	CPMG
FOV [mm^3]	$256 \times 256 \times 80$	$256 \times 256 \times 80$	$256 \times 256 \times 1$	$256 \times 256 \times 8$	$256 \times 256 \times 8$	-	-
Resolution [mm^3]	$2 \times 2 \times 2$	$8 \times 8 \times 8$	$2 \times 2 \times 6$	$2 \times 2 \times 6$	$2 \times 2 \times 6$	-	-
FAs [°]	5.4772, 9.6549, 17.019, 30.0	60	90, 180	180, 90, 180	90, 180	180,90	90, 180
TE/ES [ms]	4	4	32 steps, ranging from 15 to 480	15	32 steps, ranging from 15 to 480	-	20 steps ranging from 1 to 5000
TI [ms]	-	-	-	50, 100, 200, 400, 800, 1600, 4500	-	20 steps ranging from 6 to 6000	-
TR [ms]	23	32, 96	5000	5000	5000	10 000	10 000
Scan time [h:m:s]	00:19:38	00:04:02	00:10:40	01:14:40	05:41:20	01:59:43	01:31:22
Tread [ms]	6.4	6.4	6.4	6.4	6.4	-	-

Abbreviation: FOV, field of view.

six-element body coil was wrapped around the phantom (shown in Figure S1).

T1 and T2 measurements in both the $NiCl_2$ and $MnCl_2$ arrays were made using two protocols: a standard spin echo protocol (approximately 7 h) and an abbreviated protocol (approximately 35 min), both implemented in Pulseq.[21] All sequence details are provided in Table 1. The standard spin echo protocol consisted of inversion-recovery spin-echo (IRSE) and single-echo spin-echo (SESE) sequences, with one exception. For the commercial system, due to a bug in the sequence development framework at the time of the study, product SESE was used for SESE T2 measurement, instead of Pulseq SESE. For the abbreviated protocol, a 3D variable flip angle gradient echo (VFA-GRE) sequence was used for T1 mapping, and measurements were made of $MnCl_2$ and $NiCl_2$ arrays simultaneously. The same VFA-GRE sequence with flip angle (FA) 60°, TRs 32 and 96 ms was used for actual FA imaging (AFI).[22,23] The B1 maps were used to calculate actual FAs for fitting T1 via VFA-GRE. A 2D multi-contrast spin-echo (MCSE) sequence was implemented in Pulseq for T2 mapping. Two slices were acquired to cover both the $MnCl_2$ and $NiCl_2$ arrays. The Pulseq pulse sequences are available at https://github.com/usc-mrel/PulseqT1T2Mapping. The standard spin echo protocol measurements were acquired once, and the abbreviated protocol measurements were acquired three times on each system during the study time frame.

The acquired images were reconstructed using Gadgetron[24,25] and then quantitative MRI maps constructed using qMRLab[16] and StimFit[12] (open-source frameworks available for MATLAB). Raw data from the scanner were converted to the magnetic-resonance raw data (MRD) format.[26] Following the application of a fast Fourier transform (FFT) reconstruction in Gadgetron, the background was masked with convex-hull based masking, using MATLAB's bwconvhull function, to speed up processing time and make online visualization easier (MATLAB R2021a, Mathworks, Natick, MA, USA). Open-source qMRLab[16] was used on the masked images to calculate T1 and T2 values from the IRSE, SESE, and VFA-GRE data. B1 maps acquired with AFI were used for calculating voxel-wise actual FAs for fitting T1 VFA-GRE, also using qMRLab. T2 maps based on the MCSE sequence were estimated using the StimFit[12] package, which accounts for stimulated echoes. Region of interest (ROI) masks for the vials in the $NiCl_2$ and $MnCl_2$ arrays were applied to the processed T1 and T2 maps.[8] The vial masks were eroded by two pixels to avoid effects of partial volume, and individual voxels were used for the data analysis. For the 3D VFA-GRE acquisition, two slices through the center of the vials were included in the ROI. The reconstruction and

mapping code is available at https://github.com/usc-mrel/PulseqGadgetronRecon.

At one prototype 0.55T system, the SESE acquisition on the $MnCl_2$ array was incomplete; only the first 21 echoes of the 32 prescribed echoes were acquired. The reported results for that measurement use only these 21 echoes instead of the full dataset. No data were excluded from the analysis.

2.2 | NMR-reference measurements at 0.55T

Reference measurements were made at 0.55T using a variable field NMR system (Tecmag Redstone console, TNMR software) and a custom RF probe that allowed sample temperature control at 20°C. Measurements were made on a subset of witness samples from the same batch of $NiCl_2$ and $MnCl_2$ solutions used in the system phantom. In total, 18 samples were measured: 9 from each of the $NiCl_2$ and $MnCl_2$ arrays. A subset of these measurements was previously reported.[27]

NMR-reference T1 was measured using inversion recovery protocols with composite 180-degree pulses; NMR-reference T2 was measured using a Carr-Purcell-Meiboom-Gill (CPMG) pulse sequence. T1 was calculated using:

$$S_i = S_0 * \left(1 - (1 + d) * e^{(-TI/T1)}\right) \quad (1)$$

where T1 is the target value to fit, TI the inversion time, d a scaling factor for imperfect inversion, S_0 the nominal signal intensity, and S_i the measured signal intensity. Similarly, T2 was calculated using:

$$S_i = S_0 * e^{(-TE/T2)} \quad (2)$$

where T2 is the target value to fit, and TE the echo time.

Across both the subset of $NiCl_2$ and $MnCl_2$ arrays, the measured values ranged from 66 ms to approximately 1550 ms for T1 and 41 ms to approximately 915 ms for T2 (Table S1).

2.3 | In vivo measurements

Five healthy participants were imaged at each site under protocols approved by the Institutional Review Board of each institution, after providing written informed consent. Participants were independently recruited at each site. All participants were women between the ages of 22 and 29 y old. Specifically, at Prototype 1 participants were ages 24–29 y old (mean 26 y old, SD 2.1 y). At Prototype 2 and Commercial 1, participants were 24–28 y old (mean 26.1 y, SD 1.6 y). Finally, at Commercial 2 participants were 22–29 y old (mean 26.2 y, SD 2.6 y).

The abbreviated Pulseq protocols used for in vivo measurements are detailed in Table 1. Axial data were acquired over the whole brain for the T1 and B1 measurements, and for T2 measurement a single 2D axial slice was acquired. As described in the section on phantom measurements, the images were reconstructed and quantitative T1 and T2 calculated.

2.4 | Data analysis

For the phantom MRI measurements and NMR-reference measurements, all comparisons were performed across vials 3–11 of both the $MnCl_2$ and $NiCl_2$ arrays; these vials represent a physiological range of values at 0.55T. Comparisons were made, via percent bias (%-bias), between (1) the standard spin-echo measurement and 20°C NMR-reference data and (2) the abbreviated protocol and 20°C NMR-reference data. Additionally, the coefficient of variation was calculated for each system's three repetitions of the abbreviated protocol. An analysis of variance (ANOVA) analysis (SciPy, Python) was completed to compare the abbreviated protocol mean T1 and T2 measurements (vials 3–11) from the prototype and commercial systems. Statistical significance was assessed using $p < 0.05$.

For the participant data, T1, B1, and T2 measurements are reported as probability density function histogram of values over the brain volume or single slice, respectively. The T1 histograms are filtered to values between 0 and 3000 ms and the bin width is 25 ms. The B1 histograms are filtered to values greater than 0.01, and the bin width is 0.02 (relative to a desired FA of 1.0). The T2 histograms are filtered to values between 0 and 400 ms, and the bin width is 10 ms. The bin widths show the distribution of relaxation times and are approximately square root of the total counts divided by 10. For the quantitative biomarkers T1 and T2, the location of the histogram peak and the general shape of the histogram can be compared across systems. An ANOVA analysis (MATLAB 2023b, Mathworks, Natick, MA, USA) was used to compare the difference in means for the measured T1 and T2 relaxation times between the prototype and commercial systems, and statistical significance was assessed using $p < 0.05$.

3 | RESULTS

Phantom and in vivo measurements were completed on the two prototype and two commercial systems using the

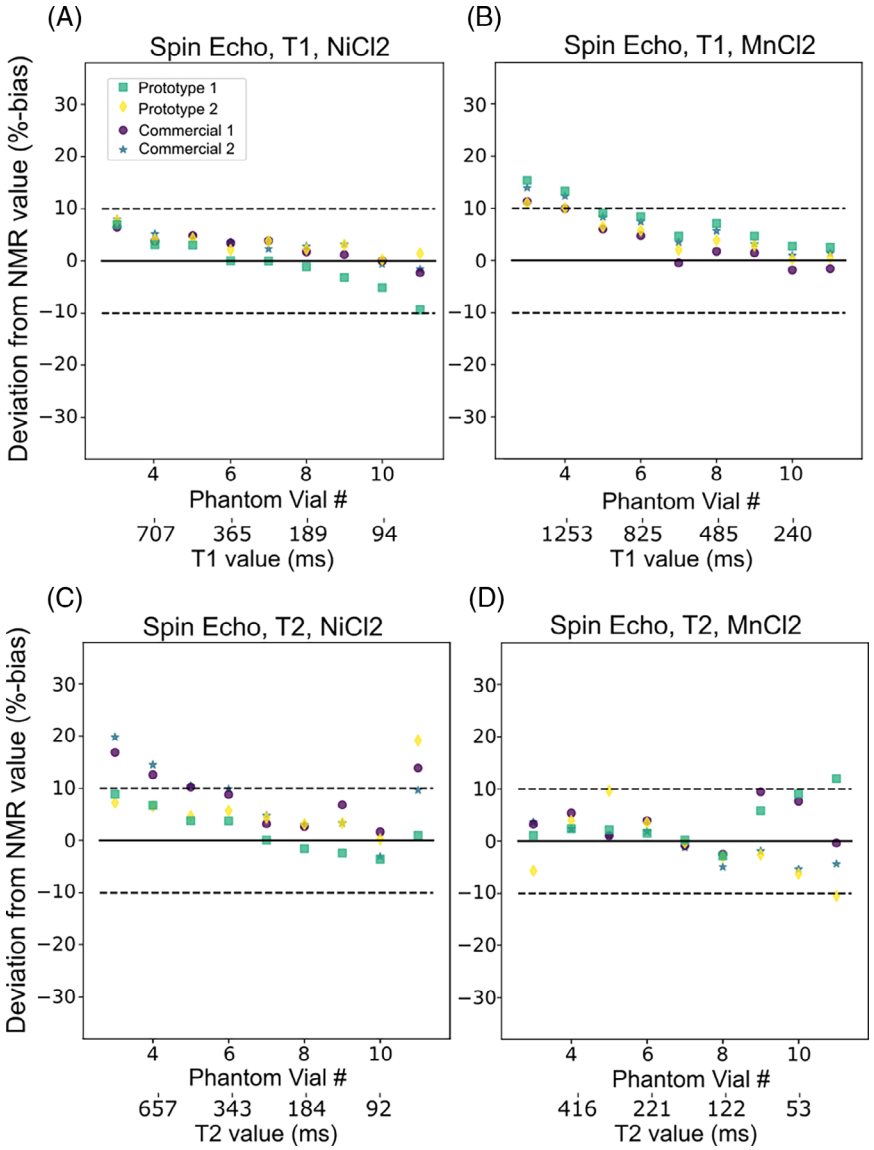

FIGURE 1 Plots of the %-bias from the NMR-reference measurement for the T1 and T2 measurements via the 7-h standard spin echo protocols (IRSE and SESE) in the $NiCl_2$ and $MnCl_2$ arrays of the ISMRM/NIST system phantom. The black solid line is 0%-bias, and the dashed lines indicate +/− 10%-bias. The majority of the measurements using the spin echo protocols are within +/− 10%-bias from the NMR-reference measurement.

open-source vendor-neutral Pulseq protocols and reconstruction pipeline (Figure S2). On Prototype 1, the phantom and in vivo measurements were completed in 12 days. On Commercial 2, the phantom and in vivo measurements were completed in 15 days. On Prototype 2 and Commercial 1, the in vivo measurements were completed in 6 days; however, the total study time frame for in vivo and phantom measurements was 30 days.

3.1 | Phantom measurements

Across all systems, the standard spin echo protocol resulted in T1 measurements in all vials in the $NiCl_2$ array which were within +/−10% of the NMR-reference measurement (Figure 1A). In general, the standard spin-echo T1 measurement of the $MnCl_2$ array was overestimated compared to the NMR-reference measurement (Figure 1B). Additionally, for $MnCl_2$ vials with long T1 times, the %-bias was up to 15%. The standard spin echo T2 measurement of $NiCl_2$ generally overestimated compared to the NMR-reference measurement and the %-bias was up to 20% (Figure 1C). Finally, for T2, the standard spin echo measurement of the $MnCl_2$ array was within +/−10% of the NMR-reference measurement except for two vials (Figure 1D).

Using the abbreviated protocol, the T1 measurement for both the $NiCl_2$ and $MnCl_2$ arrays were within approximately +/−30%-bias from the NMR-reference measurement (Figure 2A,B) except for two $NiCl_2$ measurements on one commercial system (Figure S3). The abbreviated protocol included B1 measurement for the calculation of T1. For three systems, the mean measured B1 (relative to a desired FA of 1.0) for the $MnCl_2$ array varied from 0.87–1.02, while for the $NiCl_2$ array it was lower, varying from 0.67 to 0.84 (Table S2). For the Prototype 1

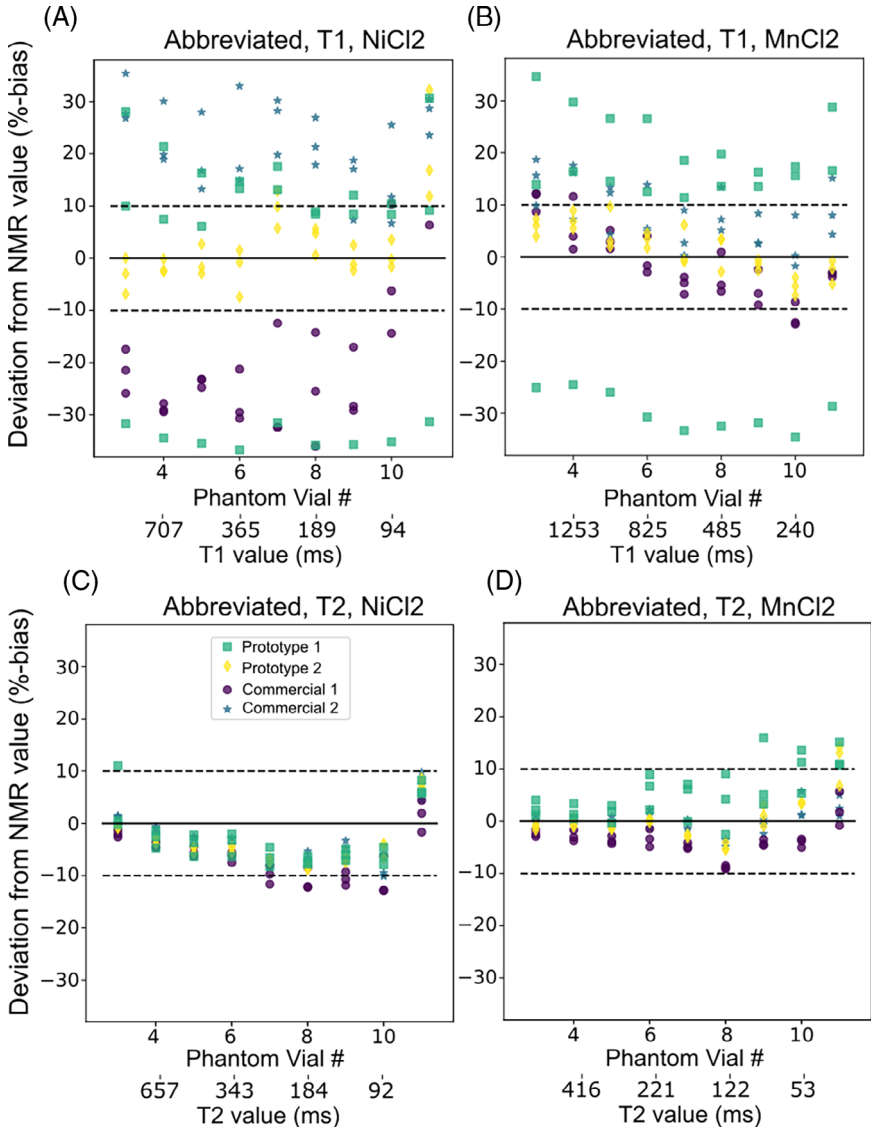

FIGURE 2 Plots of the %-bias from the NMR-reference measurement for the T1 and T2 measurements via the 35-min abbreviated protocols (VFA and MCSE) in the $NiCl_2$ and $MnCl_2$ arrays of the ISMRM/NIST system phantom. These measurements were repeated three times on each system. The black solid line is 0%-bias, and the dashed lines indicate +/− 10%-bias. Two measurements from Commercial system 1, vial 11 are not shown here (they are shown in Figure S3); these measurements were greater than 100%-bias. The abbreviated T1 measurement in the phantom has a large variability, while the abbreviated T2 measurements are mostly within +/− 10%-bias.

system, there was less difference in measured B1 between the $NiCl_2$ and $MnCl_2$ arrays. Also on Prototype 1, one B1 measurement was much greater than the other two repetitions, resulting in mean value across the $NiCl_2$ and $MnCl_2$ arrays of 1.22+/−0.26 and 1.24+/−0.21, respectively. For comparison, the next highest mean B1, across all systems and repetitions, was 1.02+/−0.17. The T2 results for both the $NiCl_2$ and $MnCl_2$ arrays were largely within +/−10%-bias from the NMR-reference measurement (Figure 2C,D).

The abbreviated protocol T1 measurement repetitions had a wide range of coefficients of variations (Figure 3A,B). For the $NiCl_2$ array, in particular, the shorter T1 vials, the coefficient of variation was greater than 5% and as large as 35% (Figure 3A). Prototype 1 had a high coefficient of variation, approximately 25% across all measurements. Excluding Prototype 1, the coefficients of variation for T1 measurement of the $MnCl_2$ array was <5% (Figure 3B). The abbreviated protocol was repeatable for T2, with coefficients of variation of <5% across all $NiCl_2$ and $MnCl_2$ measurements in vials 3–11 (Figure 3C,D).

Finally, the temperature measurements of the phantom are reported in Table 2. The temperature is reported as the average and SD of the pre- and post-scan session temperatures. Both measurements were not always recorded. For some systems and sessions, only the pre-session temperature was recorded. For one commercial system, the average temperature recorded by a temperature logger was reported, and the SD is not available. For one measurement on a prototype system, the phantom temperature increased by approximately 4°C from the pre- to post-measurement. For the remaining sessions, across all systems, the temperature change was approximately 1°C or less during the measurement session.

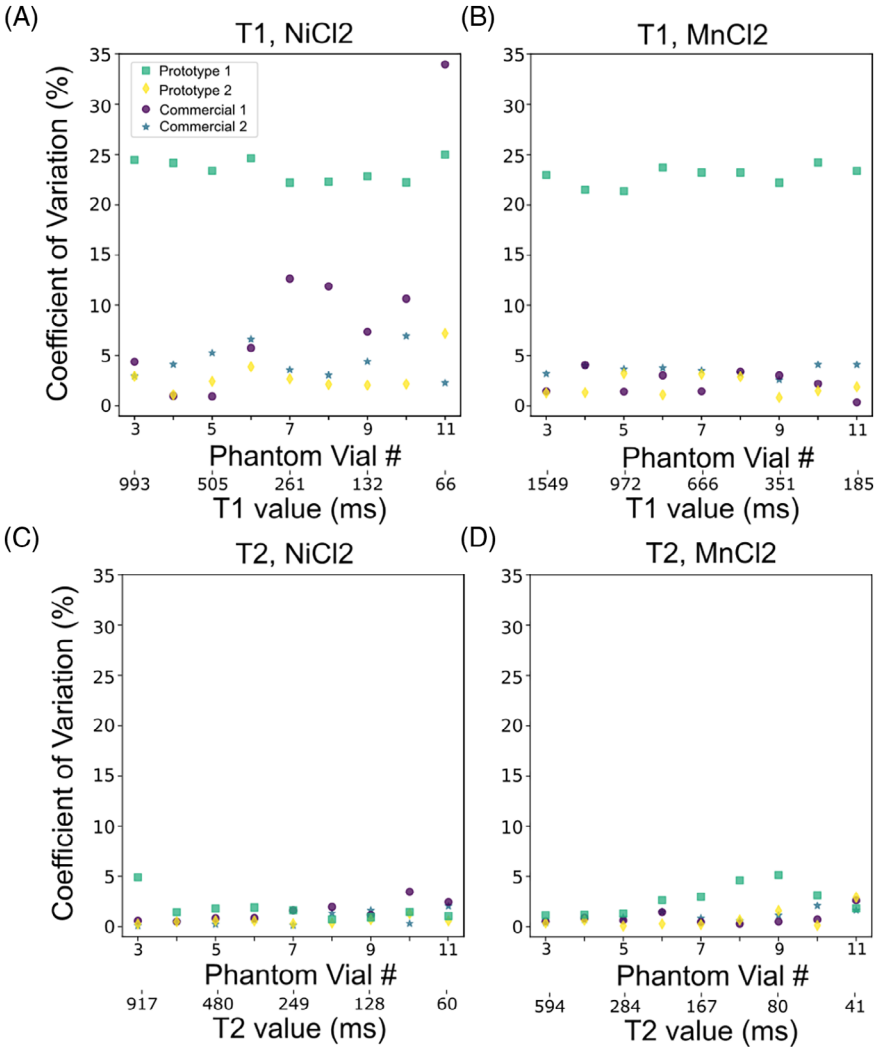

FIGURE 3 Coefficient of variation for the repeated measurements of the abbreviated protocol of the T1 and T2 measurements of the $NiCl_2$ and $MnCl_2$ arrays at each of the four systems. The Prototype 1 system has a high coefficient of variation due to a high B1 map measurement on one of the three measurements, which affected the T1 measurement. The coefficient of variation for all T2 measurements across all systems is approximately 5% or less.

TABLE 2 Phantom temperature at the time of MRI measurements.

	Prototype 1		Prototype 2		Commercial 1		Commercial 2	
	Phantom	**Ambient**	**Phantom**	**Ambient**	**Phantom**	**Ambient**	**Phantom**	**Ambient**
1	22.25 (2.99)	23.84 (0.06)	19.44 (0.15)	19.35 (pre)	19.70 (pre)	18.28 (pre)		19.66 (NA)
2	24.37 (0.41)	24.05 (0.01)	18.67 (0.19)	18.17 (pre)	18.80 (0.11)	18.42 (0.10)		19.98 (NA)
3	20.13 (0.32)	21.79 (0.65)			19.13 (0.28)			20.68 (NA)

Note: Temperature in°C reported at each system at the time of phantom measurements. Temperatures were measured of the phantom and/or of the ambient temperature in the scan room. The temperature is reported as the average and SD of the pre- and post-scan session temperatures. Both measurements were not always recorded.
Abbreviations: NA, not applicable.

3.2 | In vivo measurements

Histograms of the measured T1, B1, and T2 values across all participants and systems are shown in Figure 4. The T1, B1, and T2 histograms include all brain tissues; these are not segmented for white or gray matter. The histograms from a single system and across all systems have similar shapes and overlapping ranges of values. Across the T1 histograms, the peak location is 496 ms +/− 34 ms. For all T2 histograms, the histogram peak is typically located at 95 ms ($n = 14$), with some peaks at 85 ms ($n = 2$) or 105 ms ($n = 4$). Representative T1, B1, and T2 map slices of a representative participant from each system are shown in Figure 5. The mean B1 (relative to a desired FA of 1.0) measured in participants across all systems and participants was 0.96 +/− 0.10 (Table S3).

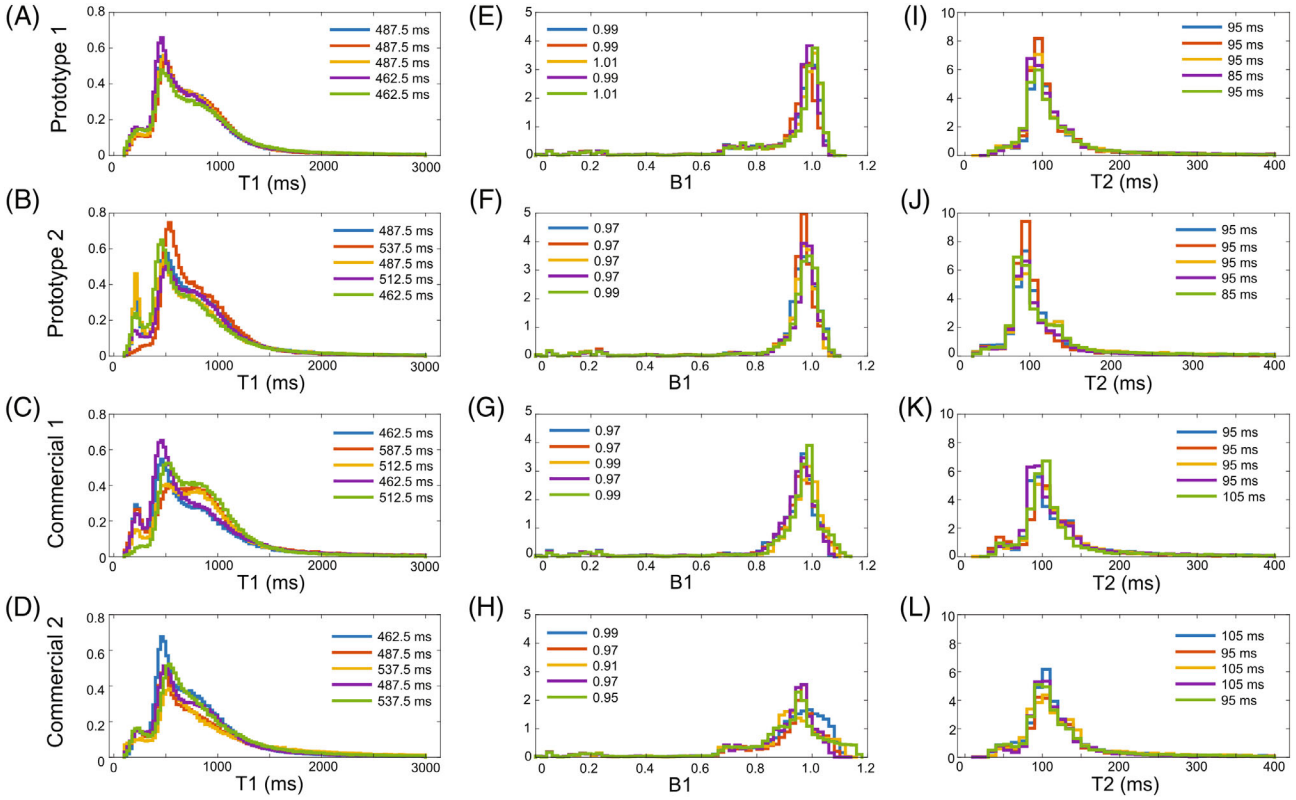

FIGURE 4 Histograms of the in vivo measured T1 and T2 values across all 20 participants at all four systems (different participants are plotted in different colors for each system). The location of the histogram peak for each participant is given in the legend. For each measurement, the histograms across all systems have similar shapes and overlapping ranges of values. Please note, the T2 map was acquired on a single slice, whereas the T1 map was acquired over the entire volume. As a result, the T2 histogram is coarser than the T1 histogram.

3.3 | Comparison of prototype and commercial systems

There was no difference in the mean brain T1 and T2 relaxation times between the prototype and commercial systems (ANOVA, T1 $p = 0.254$ and T2 $p = 0.533$). There were no significant differences between the prototype and commercial systems across all phantom measurements using the abbreviated protocol (Table 3).

4 | DISCUSSION

The purpose of this study was to assess the accuracy and reproducibility of T1 and T2 measurements on different 0.55T MRI scanners. Vendor-neutral Pulseq protocols were implemented and deployed across two commercial and two prototype 0.55T systems; these protocols and reconstruction code are freely available. There were no statistically significant differences between abbreviated phantom T1 and T2 measurements on the commercial and prototype 0.55T MRI systems. Additionally, the participant T1 and T2 measurements were not statistically different between the two types of systems. While there are differences in hardware and software between the commercial and prototype systems, it was possible to implement the same protocols and conduct quantitative measurements across the systems.

In this study, the phantom measurements served two purposes. First, the phantom was used to confirm correct implementation of the study protocol. The phantom was then used to characterize the performance of each system at the time of the participant measurements. The phantom measurements provided confidence in the T2 measurements and alerted the team to possible errors with the B1 measurement. Overall, there were no substantial differences in the phantom measurements across the systems and, thus, no concerns about the system performance for participant measurements.

Temperature was measured for the phantom measurements on all systems; however, one limitation of this study is that the same temperature measurement protocol was not followed. Errors due to temperature variation are typically systematic across all measurements for that session, and this type of systematic error was not observed. The majority of reported temperature variations within a

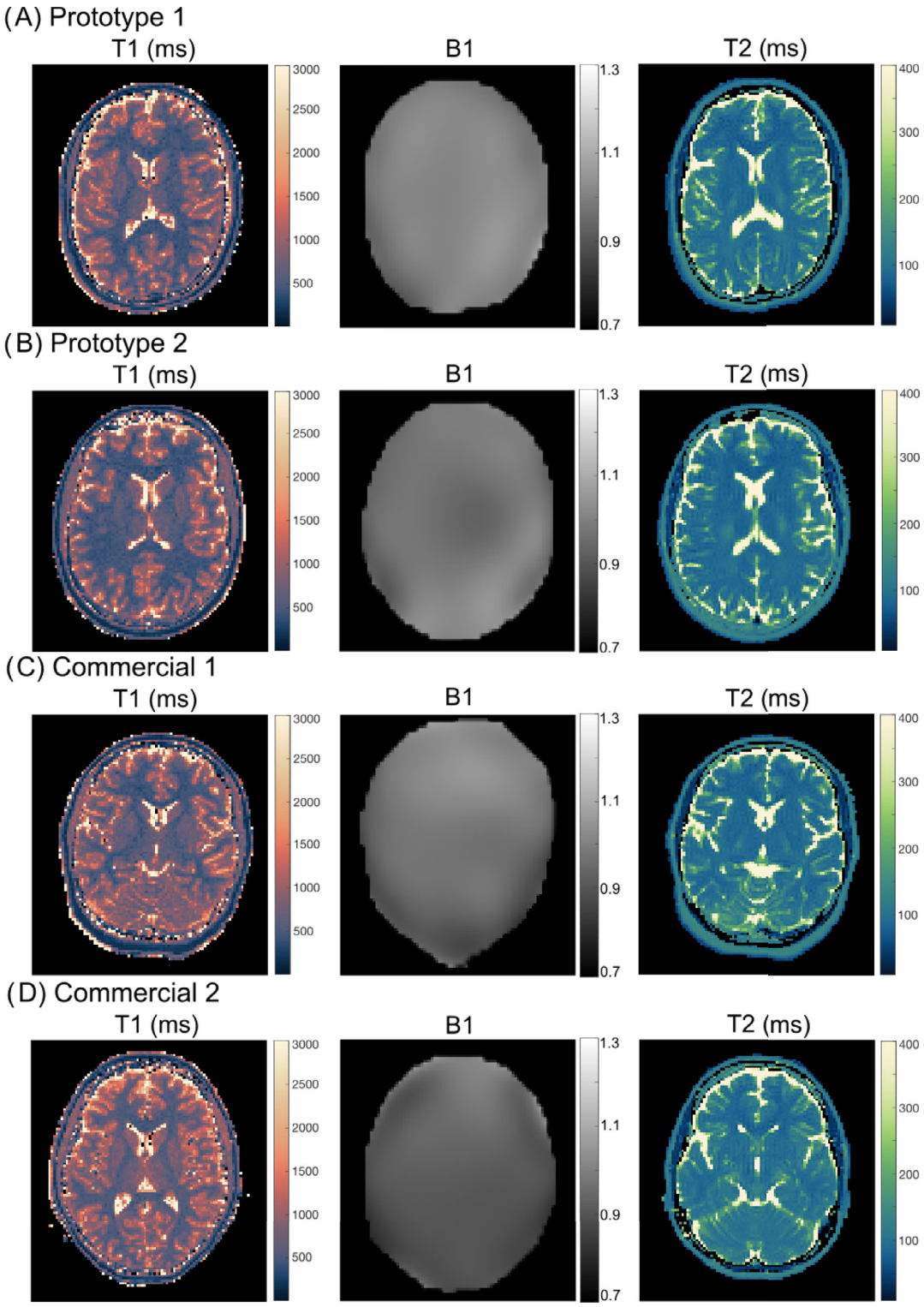

FIGURE 5 Representative maps of T1 (left), B1 (center), and T2 (right) measured in vivo from a representative participant on each system. The resulting maps are comparable across the four systems.

measurement session and across systems are sufficiently small that they are unlikely to impact the results.[28]

The multi-echo spin echo T2 measurement was highly repeatable on each system (across all vials and systems, the coefficient of variation ranged from 0.09% to 4.93% for measurements on the $NiCl_2$ array and from 0.08% to 5.16% for the $MnCl_2$ array). This is most likely due to the T2 analysis using StimFit,[12] which accounts for the stimulated echoes that can introduce error in the T2 measurement.

TABLE 3 ANOVA results (*p*-values) for comparing the T1 and T2 measured using the abbreviated protocols on the prototype and commercial systems.

	T1		T2	
Vial	$NiCl_2$	$MnCl_2$	$NiCl_2$	$MnCl_2$
3	0.623	0.308	0.309	0.800
4	0.613	0.296	0.289	0.957
5	0.690	0.306	0.304	0.910
6	0.770	0.407	0.431	0.696
7	0.898	0.515	0.651	0.786
8	0.771	0.598	0.254	0.568
9	0.603	0.538	0.757	0.376
10	0.915	0.601	0.300	0.926
11	0.669	0.759	0.680	0.348

The abbreviated protocol T1 measurement used the VFA method, which requires a B1 correction using a B1 map. In the selection of our protocol, we considered several B1 mapping methods: double angle, saturated double angle, Bloch-Siegert, and AFI. Saturated double angle did not provide accurate results due to insufficient saturation. Double angle and AFI provided consistent results; however, double angle was an order of magnitude slower than AFI and not feasible for whole-brain imaging. Finally, we chose AFI over Bloch-Siegert since AFI is easy to implement and provides fast and accurate B1 maps.

The abbreviated protocol had no statistical difference between the T1 measurements on prototype and commercial systems. However, the measurement of B1 on the Prototype 1 system was approximately 20% high for one measurement session. We do not know the cause of the B1 measurement error; possible causes include an increase in scanner temperature during that scan session or a miscalibration of the RF transmit. As a result of the B1 measurement on Prototype 1, while the majority of T1 measurements across all systems ranged from −10% to 30% bias from the NMR-reference, there is a large coefficient of variation of T1 on this system (approximately 25%), and this measurement is an outlier with a − 30% bias from the NMR-reference. Excluding the results from Prototype 1, the coefficient of variation results from the $MnCl_2$ array, 0.86% to 4.10%, are comparable to previous work.[3,4] The $NiCl_2$ array had greater variation, even when excluding the results from Prototype 1 and two outliers from Commercial 1 vial 11: the coefficient of variation ranged from 0.94% to 12.64%. This measured variability is comparable to other multi-site studies of T1 measurement via VFA.[10]

The variation in the $NiCl_2$ array is most likely due to the B1 variability at the location of the $NiCl_2$ array. When the phantom center is at isocenter of the system, the $NiCl_2$ array is located well above isocenter. For Prototype 2, Commercial 1 and Commercial 2, the phantom center was at isocenter, and the average B1 measured on the $NiCl_2$ array was 8% to 34% lower than average B1 measured on the $MnCl_2$ array. However, on the Prototype 1 system, the phantom was positioned with isocenter between the $NiCl_2$ and $MnCl_2$ arrays, and there was only a − 1% to −5% difference between the average B1 measured on the $NiCl_2$ array compared to the $MnCl_2$ array across the three repeated measurements. The discrepancy in phantom position is a limitation of the study, and future studies should specify the position of the phantom center relative to isocenter.

The 35-min abbreviated protocol was feasible for healthy participant imaging. One limitation of our in vivo study is the lack of tissue differentiation or regional analysis. For the purposes of this study, we chose to compare histograms across the entire brain and found good similarity in mean value and distribution between systems. While the phantom measurements had substantial B1 variation, this was not the case with the participant measurements. B1 was measured for each participant at the time of the T1 VFA measurements, and mean B1 measured in participants across all systems and participants was 0.94–0.98, which is consistent with the tolerance of the systems' specified transmit calibration. Other quantitative T1 measurement methods, such as MR fingerprinting,[29] are more robust to measurement errors and could be used in the future.[30,31]

We note two limitations specifically with the phantom measurements. First, the phantom did not fit in the head coil on the commercial systems. As a result, we could not use the same coil for the phantom and in vivo measurements. Second, we are unable to explain the B1 measurement error on Prototype 1. If we had recorded the pre-scan parameters, we may have observed a miscalibration on the RF transmit that would allow us to explain the measurement error.

5 | CONCLUSIONS

Quantitative T1 and T2 measurements at 0.55T in phantom (ISMRM/NIST phantom) and in vivo (healthy young adults) are not statistically different across systems when using the same vendor neutral pulse sequences, reconstruction, and analysis methods.

ACKNOWLEDGMENTS

The authors thank Maxim Zaitsev for useful input on Pulseq sequence implementation and sharing Siemens-Pulseq sequence interpreters. USC authors acknowledge research support from Siemens Healthineers and thank Mary Yung for research coordination.

University of Michigan authors acknowledge research support from Siemens Healthineers.

FUNDING INFORMATION

This study was supported by the National Institutes of Health, Intramural Research Program, National Heart Lung and Blood Institute, USA (Z01-HL006257) for NIH authors. USC authors acknowledge funding support from the National Science Foundation (1828736).

CONFLICT OF INTEREST STATEMENT

NHLBI authors are investigators on a US Government Cooperative Research and Development Agreement (CRADA) with Siemens Healthcare. Siemens participated in the modification of the MRI systems from 1.5 T to 0.55 T. Certain commercial equipment, instruments, software or materials are identified in this paper in order to specify the experimental procedure adequately. Such identification is not intended to imply recommendation or endorsement by NIST, nor is it intended to imply that the materials or equipment identified are necessarily the best available for the purpose.

DATA AVAILABILITY STATEMENT

The phantom data are available along with a representative in vivo data set: https://doi.org/10.6084/m9.figshare.25892944. The Pulseq pulse sequences are available at https://github.com/usc-mrel/PulseqT1T2Mapping. The reconstruction and mapping code is available at https://github.com/usc-mrel/PulseqGadgetronRecon.

ORCID

Kathryn E. Keenan https://orcid.org/0000-0001-9070-5255
Bilal Tasdelen https://orcid.org/0000-0001-6462-3651
Ahsan Javed https://orcid.org/0000-0003-1311-1247
Adrienne E. Campbell-Washburn https://orcid.org/0000-0002-7169-5693
Krishna S. Nayak https://orcid.org/0000-0001-5735-3550

REFERENCES

1. Li B, Lee NG, Cui SX, Nayak KS. Lung parenchyma transverse relaxation rates at 0.55 T. *Magn Reson Med*. 2023;89:1522-1530.
2. Campbell-Washburn AE, Ramasawmy R, Restivo MC, et al. Opportunities in interventional and diagnostic imaging by using high-performance low-field-strength MRI. *Radiology*. 2019;293:384-393.
3. Weiskopf N, Suckling J, Williams G, et al. Quantitative multi-parameter mapping of R1, PD(*), MT, and R2(*) at 3T: a multi-center validation. *Front Neurosci*. 2013;7:95.
4. Gracien R-M, Maiworm M, Brüche N, et al. How stable is quantitative MRI? – assessment of intra- and inter-scanner-model reproducibility using identical acquisition sequences and data analysis programs. *Neuroimage*. 2020;207:116364.
5. Captur G, Gatehouse P, Keenan KE, et al. A medical device-grade T1 and ECV phantom for global T1 mapping quality assurance-the T1 mapping and ECV standardization in cardiovascular magnetic resonance (T1MES) program. *J Cardiovasc Magn Reson*. 2016;18:58.
6. Bane O, Hectors SJ, Wagner M, et al. Accuracy, repeatability, and interplatform reproducibility of T1 quantification methods used for DCE-MRI: results from a multicenter phantom study. *Magn Reson Med*. 2018;79:2564-2575.
7. Stikov N, Boudreau M, Levesque IR, Tardif CL, Barral JK, Pike GB. On the accuracy of T1 mapping: searching for common ground. *Magn Reson Med*. 2015;73:514-522.
8. Keenan KE, Gimbutas Z, Dienstfrey A, Stupic KF. Assessing effects of scanner upgrades for clinical studies. *J Magn Reson Imaging*. 2019;50:1948-1954.
9. Boudreau M, Karakuzu A, Cohen-Adad J, et al. Repeat it without me: crowdsourcing the T_1 mapping common ground via the ISMRM reproducibility challenge. *Magn Reson Med*. 2024;92:1115-1127.
10. Keenan KE, Gimbutas Z, Dienstfrey A, et al. Multi-site, multi-platform comparison of MRI T1 measurement using the system phantom. *PLoS One*. 2021;16:e0252966.
11. Lee Y, Callaghan MF, Acosta-Cabronero J, Lutti A, Nagy Z. Establishing intra- and inter-vendor reproducibility of T1 relaxation time measurements with 3T MRI. *Magn Reson Med*. 2019;81:454-465.
12. Lebel RM, Wilman AH. Transverse relaxometry with stimulated echo compensation. *Magn Reson Med*. 2010;64:1005-1014.
13. Majumdar S, Orphanoudakis SC, Gmitro A, O'Donnell M, Gore JC. Errors in the measurements of T_2 using multiple-echo MRI techniques. I. Effects of radiofrequency pulse imperfections. *Magn Reson Med*. 1986;3:397-417.
14. Majumdar S, Orphanoudakis SC, Gmitro A, O'Donnell M, Gore JC. Errors in the measurements of T_2 using multiple-echo MRI techniques. II. Effects of static field inhomogeneity. *Magn Reson Med*. 1986;3:562-574.
15. Hanson CA, Kamath A, Gottbrecht M, Ibrahim S, Salerno M. T2 relaxation times at cardiac MRI in healthy adults: a systematic review and meta-analysis. *Radiology*. 2020;297:344-351.
16. Karakuzu A, Biswas L, Cohen-Adad J, Stikov N. Vendor-neutral sequences and fully transparent workflows improve inter-vendor reproducibility of quantitative MRI. *Magn Reson Med*. 2022;88:1212-1228.
17. Tong G, Gaspar AS, Qian E, et al. A framework for validating open-source pulse sequences. *Magn Reson Imaging*. 2022;87:7-18.
18. Tong G, Gaspar AS, Qian E, et al. Open-source magnetic resonance imaging acquisition: data and documentation for two validated pulse sequences. *Data Brief*. 2022;42:108105.
19. Gaspar AS, Silva NA, Ferreira AM, Nunes RG. Repeatability of OPEN-MOLLI: an open-source inversion recovery myocardial T1 mapping sequence for fast prototyping. *Magn Reson Med Mrm*. 2024;30080:741-750. doi:10.1002/mrm.30080
20. Liu Q, Ning L, Shaik IA, et al. Reduced cross-scanner variability using vendor-agnostic sequences for single-shell diffusion MRI. *Magn Reson Med*. 2024;92:246-256.
21. Layton KJ, Kroboth S, Jia F, et al. Pulseq: a rapid and hardware-independent pulse sequence prototyping framework:

rapid hardware-independent pulse sequence prototyping. *Magn Reson Med*. 2017;77:1544-1552.
22. Yarnykh VL. Actual flip-angle imaging in the pulsed steady state: a method for rapid three-dimensional mapping of the transmitted radiofrequency field. *Magn Reson Med*. 2007;57:192-200.
23. Yarnykh VL. Optimal radiofrequency and gradient spoiling for improved accuracy of T_1 and B_1 measurements using fast steady-state techniques. *Magn Reson Med*. 2010;63:1610-1626.
24. Hansen MS, Sørensen TS. Gadgetron: an open source framework for medical image reconstruction. *Magn Reson Med*. 2013;69:1768-1776.
25. Xue H, Inati S, Sørensen TS, Kellman P, Hansen MS. Distributed MRI reconstruction using gadgetron-based cloud computing: Gadgetron C-bud computing. *Magn Reson Med*. 2015;73:1015-1025.
26. Inati SJ, Naegele JD, Zwart NR, et al. ISMRM raw data format: a proposed standard for MRI raw datasets. *Magn Reson Med*. 2017;77:411-421.
27. Martin MN, Jordanova KV, Kos AB, Russek SE, Keenan KE, Stupic KF. Relaxation measurements of an MRI system phantom at low magnetic field strengths. *Magn Reson Mater Phys Biol Med*. 2023;36:477-485.
28. Stupic KF, Ainslie M, Boss MA, et al. A standard system phantom for magnetic resonance imaging. *Magn Reson Med*. 2021;86:1194-1211.
29. Ma D, Gulani V, Seiberlich N, et al. Magnetic resonance fingerprinting. *Nature*. 2013;495:187-192.
30. Körzdörfer G, Kirsch R, Liu K, et al. Reproducibility and repeatability of MR fingerprinting relaxometry in the human brain. *Radiology*. 2019;292:429-437.
31. Lo W, Bittencourt LK, Panda A, et al. Multicenter repeatability and reproducibility of MR fingerprinting in phantoms and in prostatic tissue. *Magn Reson Med*. 2022;88:1818-1827.

SUPPORTING INFORMATION

Additional supporting information may be found in the online version of the article at the publisher's website.

Figure S1. Photos of the ISMRM/NIST system phantom prepared for imaging on a commercial 0.55 T system.

Figure S2. Illustration of the T1 and T2 acquisition and reconstruction pipeline.

Figure S3. Plot of the %-bias from the NMR-reference measurement for the T1 and T2 measurements via the 35-min abbreviated protocols (VFA and MCSE) in the $NiCl_2$ and $MnCl_2$ arrays of the ISMRM/NIST system phantom. This plot shows the two outlier data points from Commercial system 1 on vial 11, which have greater than 100% deviation from the NMR value. These measurements were repeated three times on each system. The black solid line is 0%-bias, and the dashed lines indicate +/− 10%-bias.

Table S1. System phantom values at 0.55 T. NMR measured values for the T1 and T2 in ms of the $NiCl_2$ and $MnCl_2$ arrays of the ISMRM/NIST system phantom at 0.55 T. The reported value is the mean and standard deviation (in parentheses) at 20°C.

Table S2. Phantom measured B1. Measured B1 (relative to a desired flip angle of 1.0) of the $NiCl_2$ and $MnCl_2$ arrays of the ISMRM/NIST system phantom at 0.55 T. The mean B1 value and standard deviation are reported over the phantom slices used for the VFA-GRE measurement. Measurements are reported for the three repeated measures of the abbreviated protocol.

Table S3. In vivo measured B1. Mean and standard deviation of the measured B1 value (relative to a desired flip angle of 1.0) in participants reported for each system. The participants are not the same across all systems.

How to cite this article: Keenan KE, Tasdelen B, Javed A, et al. T1 and T2 measurements across multiple 0.55T MRI systems using open-source vendor-neutral sequences. *Magn Reson Med*. 2025;93:289-300. doi: 10.1002/mrm.30281